

Optimization of Bending-Type Ultrasonic Transducers with Rotational Symmetry using COMSOL Multiphysics

Mario Jungwirth, Michael Rabl

Wels School of Engineering, Upper Austria University of Applied Sciences

Stelzhamerstr. 23, A-4600 Wels, Austria, m.jungwirth@fh-wels.at, m.rabl@fh-wels.at

Abstract: Ultrasonic sensors are commonly used for a wide variety of non-contact presence, proximity or distance measuring applications in industry, especially the automotive branch. This paper shows how the radiation properties of bending-type ultrasonic transducers with rotational symmetry depend on shape, dimensions and material parameters. In order to determine their dependencies, the behaviour of such transducers with regard to their emitting characteristics in air was simulated using finite element (FE) methods for computing their surface elongation together with analytical elementary wave superposition. The results of the simulations have been validated by Laser Doppler Velocimetry (LDV) and angular-dependent acoustic pressure measurements.

Keywords: Bending Type Ultrasonic Transducer, Acoustic-Structure Interaction, Optimization

1. Introduction

Non-contact object detection is a necessary requirement for many object recognition applications and can be accomplished by using various wave propagation techniques, e.g. ultrasound time-of-flight measurement in accordance with the impulse-echo principle can be used, whereby a transducer transmits a short pulse of ultrasound towards the object in order to locate it. The wave is then reflected by the object and picked up by the transducer after a period of time Δt . The distance s between transducer and object can thus be determined by the speed of the transmitted wave c (for ultrasound in air under standard conditions: $c = 343$ m/s) with:

$$s = \frac{\Delta t \cdot c}{2}.$$

The time difference Δt is thereby the time between the transmission and the return of the signal.

In automotive applications bending-type ultrasonic transducers are most commonly used, because of their robustness, low cost, relatively

high sensitivity to acoustic pressure and sufficient sharpness of directivity.

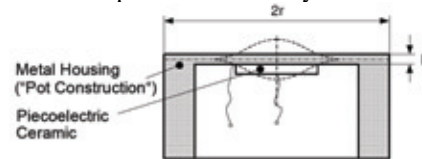


Figure 1: Closed-construction design of a bending-type ultrasonic transducer with an indication of fundamental resonance front deformation [1]

In Fig. 1 the construction is shown in principle [1]. Such an ultrasonic transducer consists of a piezoelectric element bonded to a thin, flexible metal diaphragm with thickness h . This composite forms the actual bending element, the so called bimorph. When an alternating voltage is applied to the piezoelectric ceramic disk, it deforms periodically, causing the metal diaphragm to bend (schematically shown as dashed lines).

If the mechanical resonance frequency of the ceramic/metal element and the frequency of the applied voltage match, the amplitude of the vibrations and, accordingly, the sound output to the surrounding air will be at a maximum. In Fig. 2 the characteristic of the electrical impedance over the frequency can be seen. The two peaks indicate the resonance- and anti-resonance frequency of the transducer.

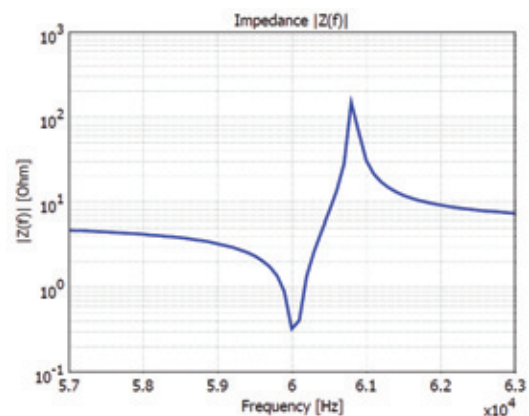


Figure 2: Electrical impedance over frequency

The electrical behaviour of such a resonator can be described using the electromechanical coupling caused by the piezoelectric effect.

In Fig. 3 the electrical circuit equivalent of a piezoelectric ceramic transducer is depicted, where C_0 denotes the static capacitance of the ceramic element, C_m the capacitance (compliance) and L_m the inductance (mass) of the mechanical circuit and R_m the resistance caused by mechanical losses (damping) [2].

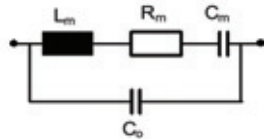


Figure 3: Electrical circuit equivalent of a piezoelectric ceramic transducer [2]

In impulse-echo applications the transmitter and receiver functions are accomplished by the same bending-type ultrasonic transducer, therefore its directivity is of major importance. In the far field the directivity depends on the wavelength λ of the emitted ultrasonic wave in the air, the diameter of the area that is radiating the signal and the local amplitude distribution within this area [1].

In Fig. 4 the directivity (logarithmic scale) of an ultrasonic transducer with completely homogeneous front surface displacement (“plane piston”-movement) in the far field is shown. One recognizes that, using this idealized type of transducer, a regularly shaped ultrasound beam with two smaller side lobes is obtained. This is, for instance, the working principle of the sensor used in proximity-warning devices such as parking aids. Therefore it is an important objective in transducer development to achieve a plane piston displacement of the transducer surface.



Figure 4: Directivity (logarithmic diagram) of a plane piston in the far field [1]

The angle α describes the total angular width of the main beam and indicates the angle range for which a) the loss in the acoustic pressure during transmission or, respectively, b) the microphone sensitivity during reception is smaller than 6 dB in relation to the 0° direction.

The diaphragm mass determines the acoustic impedance match between the bending-type transducer and the surrounding medium (air) and substantially affects the attainable surface displacement. A low diaphragm mass leads to a larger surface displacement and thus to an increase in acoustic pressure. Therefore density and stiffness (expressed by the modulus of elasticity) of the diaphragm material are the main criteria for the choice of material. In the literature similar material aspects can be found for the static mode (piezoelectric flexional actuators). This relates in particular to the elasticity and density of the passive element [3].

2. Finite Element Model

The numerical simulations were performed with COMSOL Multiphysics 3.5a using coupled analysis (acoustic-structure interaction) employing the application modes `smplx` and `acpr`. The simulation results were compared to the results from ANSYS. Figure 5 shows the elements of the bending-type transducer model, which assumes a rotational symmetry at $r = 0$. The essentials of the construction are the flat-parallel front diaphragm with a lateral stabilization ring (here pot construction), the piezoelectric ceramic disk as the driving element and a damping material located on the rear of the unit.

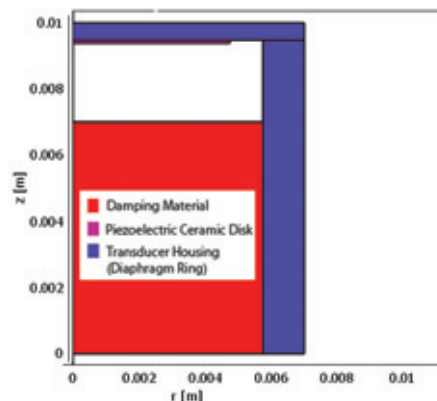


Figure 5: Finite Element Model of a closed design bending-type transducer (“pot construction”)

For numerical simulations the appropriate material parameters are assigned to the different types of subdomains [4]. After that, an alternating voltage is applied and the local displacements and the total acoustic pressure, themselves dependent on the voltage frequency, are computed.

3. Acoustic Field Computation

From the diaphragm displacements the associated acoustic field is calculated using elementary wave superposition (“Huygens principle”).

According to Huygens principle, the infinitely small areas dS of the transducer front radiate elementary waves, which establish the partial acoustic pressures $d\underline{p}$ at point P . The total acoustic pressure \underline{p} can then be calculated by integration over the entire transducer surface [5].

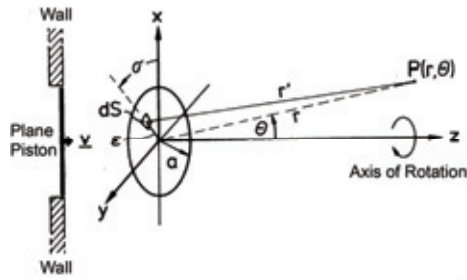


Figure 6: Acoustic field contribution of the infinitely small areas dS of the transducer front at point P [5]

Due to the rotational symmetry assumed for the geometry the local dependencies can be described completely using two cylindrical coordinates (r, θ) . According to Fig. 6 the far field can be determined analytically as the total acoustic pressure \underline{p} by superposition of the partial acoustic pressures $d\underline{p}$, whereas the approximation $r' \approx r$ for the absolute value and $r' \approx r - \varepsilon \sin\theta \cos\sigma$ for the argument can be used.

The total acoustic pressure \underline{p} can be obtained performing an integration of the partial acoustic pressures over the front surface \underline{S} . With J_0 as the Bessel function of the zeroth order the summation of the differential contributions of the ring elements results in the angular-dependent acoustic pressure

$$\underline{p}(r, \theta) = j \frac{Z_0 k}{2\pi r} e^{j(\omega t - kr)} \sum_{i=1}^N \varepsilon_i v(\varepsilon_i) 2\pi J_0(k \varepsilon_i \sin \theta) \Delta \varepsilon,$$

where v denotes the radial local velocity of the transducer front, ε the radius of the ring segments, σ the angle of the cylindrical coordinates and $k = 2\pi/\lambda$ the wave number and $N = a/\Delta\varepsilon$ the number of ring elements according to the intersection chosen.

In COMSOL Multiphysics the total acoustic pressure can be calculated and evaluated alongside certain boundaries. In this work the total acoustic pressure $\underline{p}(r, \theta)$ is to be evaluated along a semi-circle. Due to the rotational symmetry of our model only a quadrant is evaluated.

In Fig. 7 the height plot of the total acoustic pressure is shown. In order to truncate the infinite surrounding domain, perfectly matched layer (PML) elements are used in the outermost domain.

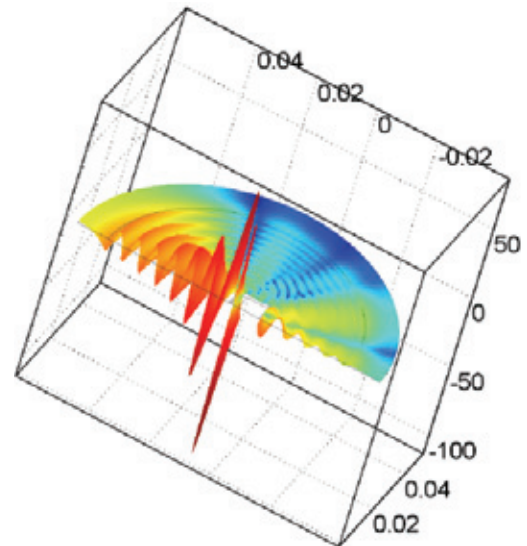


Figure 7: Height plot of total acoustic pressure with surrounding PML-elements

4. Experimental Setup

Based upon these simulation results prototype transducers were developed and their characteristics have been examined experimentally by angular dependent microphone measurements and by Laser Doppler analysis of the surface displacements [6].

The Laser Doppler Velocimetry (LDV) enables a contactless measurement of the surface displacements of the sample under test. The laser beam is thereby focused on the diaphragm of the bending-type transducer, where it is back-

scattered at the vibrating surface. Depending on the speed of the diaphragm deflection, the reflected light experiences a change of frequency and phase which thus represents the motional information.

With the angular dependent microphone measurement the acoustic field was measured by incremental angular displacement of the ultrasonic transducer and also using a calibrated measuring microphone.

The surface displacements and acoustic pressures obtained by the numerical simulations were compared to the real behaviour of the prototype transducers, whereby conclusions about possible improvements of the transducer characteristics could be drawn.

5. Validation of the Computer Models

The variation of the geometry parameters during the various transducer simulations has lead to a 60 kHz transducer made of aluminium (diaphragm and stabilization ring) with an outer diameter of 14 mm and a wall thickness of 1,25 mm which shows the expected characteristics regarding on-axis acoustic pressure, microphone sensitivity and directivity respectively. Such a transducer was analyzed in detail using microphone measurement and LDV.

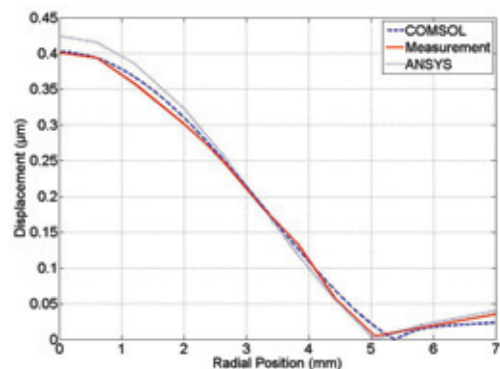


Figure 8: Displacement of diaphragm - Simulation vs. Measurement

The simulation results with COMSOL and ANSYS fit very well with the measured data, as depicted in Fig. 8 and Fig. 9. This means that FE modelling can be seen as a very effective tool for optimizing a bending-type transducer with regard to the intended application.

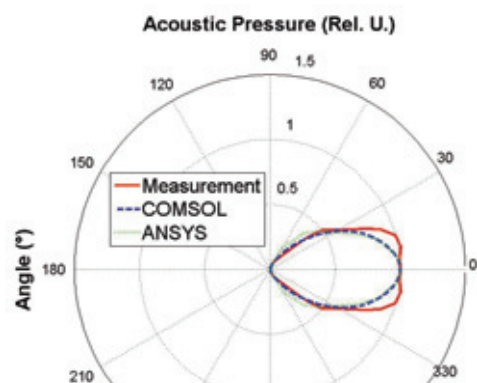


Figure 9: Angular dependence of acoustic pressure (directivity) - Simulation vs. Measurement

5.1 Height Dependence of Pot Construction

A bending-type transducer with a “closed-construction” design consists of a front diaphragm and a stabilization ring (“pot” construction). The diaphragm is responsible for the acoustic impedance matching between transducer and the air by displacing the volume as much as possible. The lateral ring as an acoustically inert mass minimizes the edge movements, which are always in opposition to the phase of the diaphragm’s centre. This is an essential goal in order to suppress interference extinctions (“plane piston approximation”).

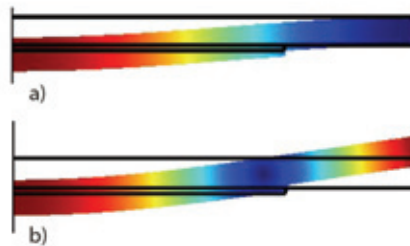


Figure 10: Diaphragm edge mounting: a) clamped, b) loose

The principal effect of the stabilization ring is demonstrated in Fig. 10. If the diaphragm edge is clamped tightly (“ideal” edge fixation), it behaves to a large extent like a plane piston emitter, i.e. all displacements are in phase (see Fig. 10 a). A diaphragm however with an edge moving freely (loose) without any stabilization, vibrates at the centre and edge in opposite directions (see Fig. 10 b). This leads in general

to unpredictable on-axis pressure levels and to pronounced side lobes in the directivity.

The stabilization ring is a rather effective approximation of a fixed edge, as can be seen from the regular shape of the angular sound pattern. A maximum of on-axis acoustic pressure can only be obtained if edge movement is minimized by the stabilization ring as seen in Fig. 11.

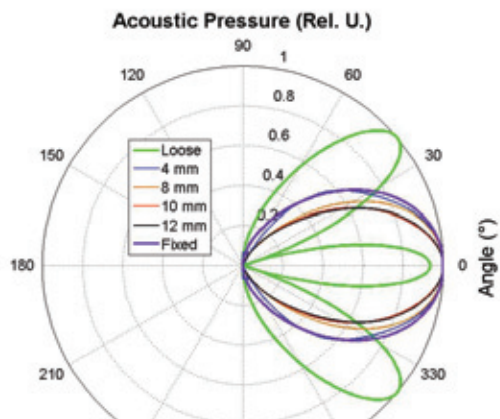


Figure 11: Angular dependence of acoustic pressure (directivity) depending on pot height and edge fixation.

Figure 11 shows how extremely irregular acoustic fields result from insufficient edge fixation.

5.2 Material Dependence

The analyses have shown that there is a potential for further improvements with respect to the efficiency of the transducer depending on the choice of material. Particularly the diaphragm determines the acoustic impedance matching between transducer and medium (air). Here the diaphragm mass is of major importance. In principle the moving mass should be as small as possible, since these results in larger surface displacements. On the other hand the impedance matching requires a certain diaphragm thickness to obtain a specific resonance frequency. Therefore density and elasticity are crucial criteria for the material choice. A particularly suitable diaphragm material should be of low density and have a high modulus of elasticity. fiber-reinforced composites can show such properties. According to [7] Carbon fiber reinforced polymer (CFRPs) have a density of

1810 kg/m³ and a modulus of elasticity of 228 GPa, which corresponds very well to the specifications required.

6. Conclusions

The FE simulations of the diaphragm displacements were performed both with COMSOL Multiphysics 3.5a and ANSYS 11. The systematic variations in geometry dimensions, e.g. diameter, height, ring and diaphragm thickness and the material properties (stiffness and density) were focused on transducers with a resonance frequency of 60 kHz. Based on the simulation data obtained, transducer variant were built. The resulting surface displacements were scanned locally with a single point laser-doppler vibrometer and the acoustic pressure was measured with a microphone positioned in relation to the angle of radiation.

From the simulations and experiments, ideal parameter settings for the design of transducers with high radiation efficiency were found. These show that, using aluminium as a standard material, an efficient, easy-to-build 60 kHz transducer of small size and adequate directivity can be made.

In view of the properties of carbon fiber reinforced polymers (CFRP) materials potentially suitable for the diaphragm due to their high stiffness and low density.

7. References

- [1] Koch, J.: *Piezooxide (PXE) Eigenschaften und Anwendung*, Valvo-Broschüre, Hamburg (1988)
- [2] Arnaud, A.: *Piezolectric Transducers and Applications*, Heidelberg (2004)
- [3] Riedel, M.: *Piezokeramische Biege wandler, Piezokeramik. Grundlagen, Werkstoffe, Applikationen*, Kontakt & Studium, Werkstoffe, Band 460 (1995), p. 153-171
- [4] Kaltenbacher, M.: *Numerical Simulation of Mechatronic Sensors and Actuators*, Heidelberg - Berlin (2007)
- [5] Zollner, M., Zwicker, E.: *Elektroakustik*, Heidelberg - Berlin (1998)
- [6] Rabl, M., Jungwirth, M., Zeller, P.: *Development of Bending-Type Ultrasonic Transducers with Rotational Symmetry*, SENSOR 2009 Proceedings II, p. 247 – 252
- [7] Callister, W. D. Jr.: *Fundamentals of Material Science and Engineering*, New York (2001)